# Segmentation of EMG time series using a variational Bayesian approach for the robust estimation of cortical silent periods

Iván Olier[1], Julià Amengual[2] and Alfredo Vellido[3] *

1- Institut de Neurociències - Universitat Autónoma de Barcelona
Edifici M, Despatx M3/206, 08193, Bellaterra (Barcelona) - Spain

2- Neurodynamics Laboratory - Dept. of Psychiatry and Clinical Psychobiology
Universitat de Barcelona, 08035, Barcelona - Spain

3- Dept. de Llenguatges i Sistemes Informàtics - Universitat Politècnica de Catalunya
Edifici Omega, Campus Nord, 08034, Barcelona - Spain

**Abstract**.  A variational Bayesian formulation for a manifold-constrained Hidden Markov Model is used in this paper to segment a set of multivariate time series of electromyographic recordings corresponding to stroke patients and control subjects.  An index of variability associated to this model is defined and applied to the robust detection of the silent period interval of the signal.  The accuracy in the estimation of the duration of this interval is paramount to assess the rehabilitation of stroke patients.

## 1  Introduction

The Transcranial Magnetic Stimulation (TMS) of the cerebral motor cortex can evoke waves in the electromyographic (EMG) recording of muscle activity. Cortical stimulation can elicit excitatory as well as inhibitory effects. One of the latter is called the cortical silent period (CSP). When TMS is delivered over the motor cortex while the subjects maintain voluntary muscle contraction, the CSP is a pause in ongoing EMG activities that follows the motor-evoked potential.

The duration of the CSP is an important parameter to gauge the recovery of stroke patients and to provide them with a prognosis. It is known [1] that the shortening of the SP in the affected side is related to an increase of its excitability, indicating an improvement of the motor function of the patients. The measurement of the CSP is sometimes troublesome due to the nature of the signal. The existing measurement methods are yet imprecise and are known to yield a significant error due to the sensitivity to noise of this kind of data [2].

The main purpose of this study is to provide an accurate technique for CSP estimation based on a multivariate time series (MTS) segmentation process that behaves robustly in the presence of noise. For this, we resort to a manifold-constrained Hidden Markov Model (HMM). The formulation of this model within a variational Bayesian framework imbues it with regularization properties that minimize the negative effect of the presence of noise in the EMG MTS. A novel index of variability ($IV$) is defined for this model. It is capable of providing reliable estimates of the CSP duration by pinpointing its offset time with precision.

## 2    EMG recordings from stroke patients and controls

Motor disabilities caused by stroke have been the target of several recently developed therapies shown to be more effective than standard physiotherapeutic approaches [3]. Several basic neuroscience studies have shown that music training produces rapid changes in motor-related brain areas ([4],[5]). In Musical-Supported Therapy (MST), musical instruments are used to train motor functions in patients suffering from mild to moderate paresis after stroke.

For the current study, several chronic stroke patients were involved in MST therapy, in order to provide the first evidence, in the form of TMS-induced EMG recordings, of the possible neuroplastic changes induced by it.

Motor-evoked potentials were obtained from the first dorsal interosseus (FDI) muscle of the hand contralateral to the stimulated hemisphere. Both hemispheres were tested. CSP was registered for all subjects. Stimulation of the motor cortex in both hemispheres with contralateral voluntary FDI muscle activation, controlled with a pression gauge, was performed. EMG data corresponding to a total of 15 pulse stimulations were recorded for each subject (including several control subjects). The signal was windowed from 125 ms prior to stimulus onset to different durations. The recordings result in 15 time series for each subject.

## 3    Variational Bayesian Generative Topographic Mapping Through Time

When defined within the Statistical Machine Learning framework, manifold learning models can be made to rely in sound principles, while embodying attractive properties such as data visualization, adaptive parameter optimization and ease of extensibility. Generative Topographic Mapping Through Time, or GTM-TT [7], is one such technique, defined as a manifold-constrained HMM. It is capable of providing simultaneous clustering of MTS and their visualization in low-dimensional representation spaces. GTM-TT was recently assessed in [6].

The presence of uninformative noise in the analyzed data and the associated problem of overfitting can seriously hamper the modeling of MTS. In its basic formulation, GTM-TT is prone to overfitting unless active regularization methods are applied. The reformulation of this model within a Bayesian framework confers it with regularization capabilities in a natural way by penalizing over-complex models through the use of appropriate priors. The implementation of this Bayesian reformulation using variational techniques results in the Variational Bayesian GTM-TT (VB-GTM-TT), which has previously been shown to deal effectively with the problem of overfitting [8].

Avoiding a direct Maximum Likelihood approach, variational inference defines a lower bound for the marginal log-likelihood of the model, as

$$\ln p\left(\mathbf{X}\right) = \ln \int \sum_{\text{all } \mathbf{Z}} p\left(\mathbf{Z}, \mathbf{X}|\boldsymbol{\Theta}\right) p\left(\boldsymbol{\Theta}\right) d\boldsymbol{\Theta} \tag{1}$$

where $\mathbf{X}$ are the MTS data; $\mathbf{Z}$ are the hidden states defined by the model; and

$\Theta$ are the model parameters, including a matrix with the centroids or prototypes embedded in the model manifold $\mathbf{Y}$, initial state probabilities $\boldsymbol{\pi}$, and transition probabilities $\mathbf{A}$. These parameters depend, in turn, on a set of hyperparameters $\boldsymbol{\nu}$, $\boldsymbol{\lambda}$, $\epsilon$, $\alpha$, $d_\beta$, $s_\beta$. The complete model is graphically illustrated by Fig. 1. Details on model optimization and parameters estimation can be found in [8].
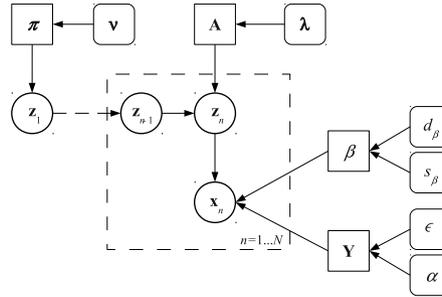


Fig. 1: Graphical representation of the Bayesian GTM-TT. Variables are noted by circles, parameters, by squares, and hyperparameters, by rounded squares.

### 3.1 Index of Variability

GTM-TT can facilitate the identification and visualization of change-points and sudden transitions in MTS [6]. Change-points, in the low-dimensional visual data representation provided by the model, correspond to sudden jumps between usually distant model states. Instead, subsequences of little variability over time will often clump in few model states or even remain in a single one over time. Beyond the MTS exploratory visualization that GTM-TT can provide, we need a well-defined measure of MTS variation to allow us to identify and quantify change-points. In GTM-TT, we expect sudden transitions to be accompanied by sudden increases of the model likelihood [6], so that the weighted mean of the emission probabilities in logarithmic form can be used as an Index of Variability ($IV$): $IV_n = -\sum_k r_{k,n} \ln p\left(\mathbf{x}_n | \mathbf{z}_n = k\right)$, where $r_{k,n}$ is the responsibility (a posterior probability) taken by a hidden state $z_n = k$ out of $K$ for each point $x_n$ in the MTS.

Unfortunately, this measure is prone to be affected by the presence of noise and, therefore, it will not reflect the advantages of the data regularization provided by VB-GTM-TT. For this reason, a novel $IV$ measure is proposed here, namely the weighted-prototype $IV$ ($wpIV$), which is defined as

$$wpIV_n = \|\Omega_n^{mean} - \Omega_{n-1}^{mean}\| \ , \tag{2}$$

where $\|\cdot\|$ is the Euclidean distance and $\Omega_n^{mean} = \sum_{k=1}^{K} \langle z_{k,n} \rangle \mathbf{y}_k$. Here, the variational parameter $\langle z_{k,n} \rangle$ plays the same role as $r_{k,n}$ plays for the standard GTM-TT, and vector $\mathbf{y}_k$; $k = 1 \ldots K$ is the data prototype of state $k$ in data space. Eq. 2 is nothing but the weighted distance between the data prototypes

441

representing two consecutive instants in the MTS, where each prototype can take at least partial responsibility for the representation of each instant of the MTS. The same distance measured between the observed data of the two consecutive instants would be of little use as any relevant information would be masked by noise. By measuring the distance using the model generated prototypes we ensure that, provided the model manages to faithfully recover the underlying structure of the MTS (and VB-GTM-TT does this by avoiding overfitting while the standard GTM-TT cannot), the true change-points will be clearly detected.
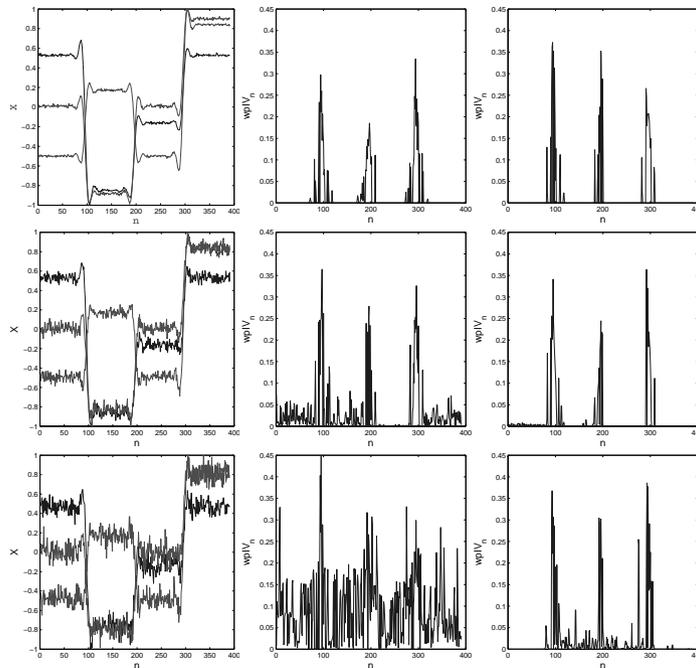


Fig. 2: $wpIV$ for the artificial data at three noise levels: 0.01 (top row), 0.05 (middle) and 0.1 (bottom). Data represented on the left column; the center column shows results for GTM-TT and the rightmost one, for VB-GTM-TT.

## 4 Experiments and discussion

The first set of experiments is meant to show the adequacy and usefulness of the $wpIV$ defined in section 3.1. For that, we model a simple artificial set of MTS using both the standard GTM-TT and the VB-GTM-TT defined in section 3. This basic dataset consists of 3 time series built as a piecewise combination of step-like functions concatenating four periods of constant signal through three sudden transition change-points. The signal is contaminated with increasing levels of uninformative Gaussian noise (Three levels with standard deviations:

0.01, 0.05 and 0.1; see Fig. 2, left column).

The *wpIV* for both models and for the three noise levels is depicted in Fig. 2 (center and right columns). At the lowest noise level (top row), the *wpIV* corresponding to both models captures both the transitions and the periods of noise-related variability. At higher levels of noise, though, only the VB-GTM-TT (rightmost column) is able to keep faithfully modelling both of them. The *wpIV* for the standard GTM-TT (center column), instead, clearly reveals that the model is overfitting the data, rendering the index useless for MTS segmentation through change-point detection.
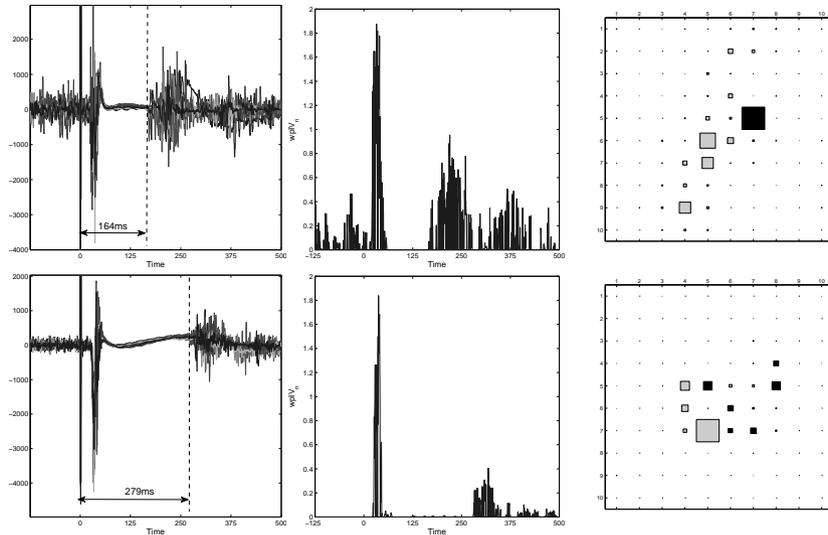


Fig. 3: Left) The 15 EMG time series for two control subjects. Dashed lines delimit the CSP durations of 164ms (top) and 279ms (bottom), estimated using the *wpIV*. Middle) *wpIV* for these subjects. Right) Visualization of the MTS in the VB-GTM-TT map. Squares represent model states and their size is an indication of the number of time points (as a ratio) assigned to each state. Such assignment takes the form of a mode-projection according to the expression $h_n^{mode} = \mathtt{argmax}_k \langle z_{k,n} \rangle$. States filled in black correspond to the CSP.

We are now in the position to turn our attention to the EMG data described in section 2 and the estimation of the CSP duration. We first provide illustrative results for two control subjects. Fig. 3 (left) shows the complete EMG of these subjects. The corresponding estimation of the *wpIV* and the MTS data visualization for VB-GTM-TT are shown in Fig. 3 (center and right, respectively). The *wpIV* provides a completely clean-cut delimitation of the CSP that allows the unambiguous estimation of its duration. The visualization in the right-hand side plot shows that the CSP is described almost in full by separate states.

The results for a stroke rehabilitation patient, displayed in Fig. 4, are con-

sistent with those obtained for the controls. Even in the presence of some rather noisy series, the CSP is neatly captured by the *wpIV*. As expected, rehabilitation shortens the CSP duration. This result encourages further research in a wider database of rehabilitation patients.
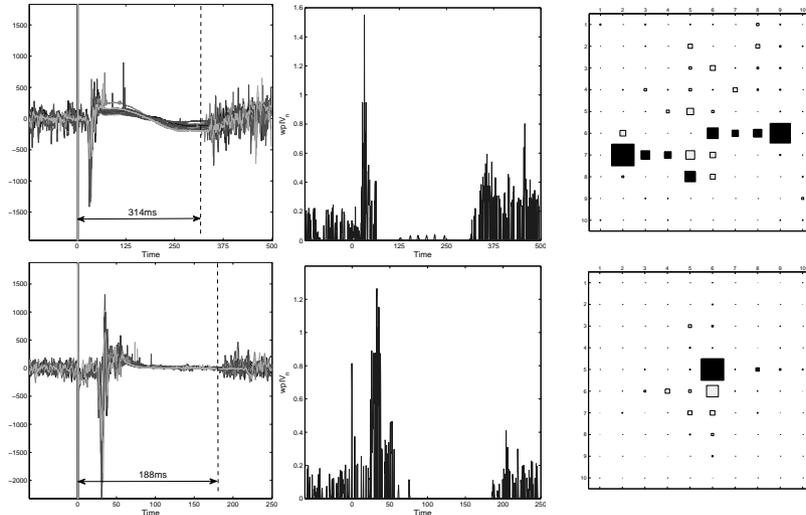


Fig. 4: Stroke rehabilitation patient. Top) Before rehabilitation; bottom) after rehabilitation. Representation as in the previous figure.

# References

[1] J. Liepert, C. Retemeyes, T. Kucinski, S. Zittel and S. Weiller, Motor strokes: The lesion location determines motor excitability changes, *Stroke*, 36:2548, AHA, 2005.

[2] Z.J. Daskalakis, G.F. Molnar, B.K. Christensen, A. Sailer, P.B. Fitzgerald and R. Chen, An automated method to determine the transcranial magnetic stimulation-induced contralateral silent period. *Clinical Neurophysiology*, 114(5):938-44, Elsevier, 2003.

[3] H. Woldag and H. Hummelsheim, Evidence-based physiotherapeutic concepts for improving arm and hand function in stroke patients: a review. *Journal of Neurology*, 249(5):518-528, Steinkopff, 2002.

[4] M. Bangert, T. Peschel, G. Schlaug, M. Rotte, D. Drescher, H. Hinrichs, H.-J. Heinze and E. Altenmüller, Shared networks for auditory and motor processing in professional pianists: evidence from fMRI conjunction. *Neuroimage*, 30(3):917-26, Elsevier, 2006.

[5] S. Baumann, S. Koeneke, C.F. Schmidt, M. Meyer, K. Lutz and L. Jancke, A network for audio-motor coordination in skilled pianists and non-musicians. *Brain Research*, 1161:65-78, Elsevier, 2007.

[6] I. Olier and A. Vellido, Advances in clustering and visualization of time series using GTM Through Time. *Neural Networks*, 21(7):904-913, Elsevier, 2008.

[7] C.M. Bishop, G. Hinton and I. Strachan, GTM Through Time. In proceedings of the IEE Fifth *International Conference on Artificial Neural Networks*, pages 111-116, U.K., 1997.

[8] I. Olier and A. Vellido, A variational formulation for GTM Through Time. In proceedings of the *International Joint Conference on Neural Networks* (IJCNN 2008), pages 517-522, Hong Kong, 2008.